International Journal of Thermal Sciences 183 (2023) 107838

Contents lists available at ScienceDirect

International Journal of Thermal Sciences

journal homepage: www.elsevier.com/locate/ijts

An experimental study to characterise the role of multihole nozzle in adjuvant assisted cryospray

Prashant Srivastava, Amitesh Kumar *

Department of Mechanical Engineering, Indian Institute of Technology (BHU), Varanasi, 221005, India

ARTICLE INFO

Keywords:
Nano-phantom
Normal-phantom
Multihole nozzle
Adjuvant

ABSTRACT

Cryospray is a process of skin cancer treatment in which liquid nitrogen is sprayed on the lesion to achieve necrosis. In order to achieve necrosis through cryospray, a combination of particular cooling rate and lethal temperature is required. The small aperture of single hole nozzle (SHN) and the less mass flow rate associated with it reduce the rate of heat transfer from the lesion. Moreover, the low thermal conductivity of lesion further reduces the rate of energy diffusion inside it. These limitations associated with the existing method of cryospray fail to provide complete necrosis in the lesions of size larger than 15 mm in diameter. The present study addresses these issues through the modification in the existing spraying technique, i.e. inclusion of multihole nozzle (MHN) in cryospray and administration of Magnesium Oxide (MgO) nanoparticles as an adjuvant in the lesion to increase its rate of energy diffusion. The influence of mass flow rate and the rate of evaporation of cryogen on cryoablation are analysed experimentally while changing the geometrical parameters of 6 MHNs. To quantify the necrosis, thermocouples and FLIR thermal imaging camera are used to ascertain temperature profile below and above the gel surface respectively. The crystalline nature of nanoparticles is confirmed through TEM and XRD results with a particle diameter ranging between 10 and 40 nm. A comparative study of cryoablation is carried out between nano-phantom and normal-phantom. An increase of 59%, 96% and 64% in the area of necrotic zone is observed on the surface of nano-phantom for MHNs with 5 holes and margin of 1 mm, 1.5 mm and 2 mm respectively. The radius of interacellular ice formation has increased by 5 mm at an axial depth of 2 mm for MHNs with 5 holes in the nano-phantom than that in normal-phantom due to the increase in cooling rate. It is also observed that nano-phantom achieves a lower end temperature than the normal-phantom at every thermocouple position. Among the 6 MHNs selected for the study, MHN with 5 holes and 1.5 mm margin provides the most optimised result with the ablation zone of 42 mm on the surface of gel. Thus, it can be concluded that because of the introduction of adjuvant and modification in spraying device, cryoablation outcomes have been improved both quantitatively and qualitatively. The proposed approach will increase the scope of cryospray in the treatment of larger lesions.

1. Introduction

Oral drug administration has drawbacks like poor drug absorption or enzymatic degradation in the gastrointestinal tract or liver. The most common alternative to oral drug administration is the painful hypodermic injection [39]. Transdermal drug administration methods (TDDAM) are always considered superior than these methods because they eliminate first pass effect [8]. But the stratum corneum (the outermost layer of skin) constrains the transport of external agents through skin; however it also saves our body from pathogens. Specially formulated drugs in terms of size, surface charge and composition are necessary to meet the requirement of transdermal transport. Therefore, there are two prerequisites of TDDAM; (i) Methods to circumvent stratum corneum and (ii) formulation of drugs. There are four physical enhancement methods to evade the stratum corneum [56]. They are microneedles, inophorosis, sonophorosis and velocity based devices. Very recently, heat based removal of stratum corneum has replaced the traditional process like tapes stripping, mechanical abrasion and chemical treatment. Since its inception from the first generation three-day patch, that delivers scopolamine to treat motion sickness, to the third generation delivery systems like microneedles, microdermabrasion etc., transdermal drug delivery has revolutionised the

* Corresponding author.
E-mail address: amitesh.mec@iitbhu.ac.in (A. Kumar).

https://doi.org/10.1016/j.ijthermalsci.2022.107838
Received 25 January 2022; Received in revised form 22 July 2022; Accepted 27 July 2022
Available online 5 September 2022

medical practice [36]. Apart from that, innovations in the field of nanotechnology has provided leverage to researchers in the synthesis of nano-meter sized specially formulated drugs for various biomedical applications [13]. Literature suggests that the pronounced effect of nanoparticles (as adjuvants) can be easily acknowledged in the field of molecular diagnostic, cancer therapy, gene delivery vehicles and anti-bacterial drug [9,38]. Nanoparticle assisted drug delivery has also gained immense popularity in dermatology; photoprotection, barrier creams, treatments of hair disorders.

The race of mankind has achieved immense advancement in the field of medical science, but an effective therapy to treat cancer remains elusive. Cancer is characterised as an uncontrolled growth of cells in any part of the body. It is responsible of 6 million casualties across the globe each year [57]. Current methods of cancer treatment like surgery, radiation, photodynamic therapy and conventional chemotherapy have certain limitations, for example whole body endure their side effects [34]. In this perspective, an alternative technique to treat cancer, termed as cryotherapy, is becoming popular nowadays. Cryotheray is further classified in two parts as cryosurgery and cryospray. Cryosurgery deals with lesions occurring inside the body whereas cryospray deals with the superficial lesions. Biocompatible nanoparticles (as adjuvants) are extensively used in the cryosurgery process for the treatment of larger lesions [24,48,65–67]. A solution loaded with nanoparticles is injected inside the tissue and enhancement in necrosis is achieved through extreme cooling. Administration of nanoparticles improves the thermal conductivity of the tissue and increase the rate of tissue destruction. Zhang et al. [63] suggested that administration of Fe_3O_4 nanoparticles inside the tissue can increase the rate of freezing leading to faster cell destruction. A study conducted on healthy male rabbit by Di et al. [15] to examine the role of MgO nanoparticles in cryosurgery revealed that nanoparticles promote and enhance the cryoinjury. Proper selection and dosing of nanoparticles are very important parameters in such studies, as they are administered in the living organisms. Yan and Liu [30] studied the impact of Fe_3O_4, diamond, carbon nanotubes and silver nanoparticles in cryosurgery through their computational model. They further reported that choosing optimal concentration with appropriate particle plays an important role in maximising the cryoablation. In the current scenario, administration of nanoparticles inside the tissue for cryosurgery is well explored by the researchers. They can be injected directly as nanofluid in the biological matrix of the tissue. However, similar approach can not be opted for cryospray, because it deals with superficial lesions and earlier trnasdermal drug transport was a challenging task. Due to this reason, adjuvant assisted cryospray is less explored in the literature.

Cryospray is a non-invasive process which employs the application of extreme cold to destroy the cutaneous cancerous tissue. Superficial lesions are treated while spraying liquid nitrogen (LN2) through a cryospray nozzle on the target tissue. It is well proven fact that skin cancers of smaller size (less than 15 mm) can effectively be treated with the cryospray process [35,49]. However, irregular and larger lesions are not treated effectively by cryospray. This is because the current practice compels surgeons to go for multiple sittings or multiple freeze-thaw cycles or overlapping fields of freezing which increase the healing time and chances of infection. For such cases, the recurrence rate is also high [12]. In addition, the current practice increases the discomfort to the patients and chances of healthy tissue destruction also persists. An in-vivo study is conducted while applying intralesional and cryospray techniques in the treatment of keloids by Mourad et al. [2]. They reported that interalesional techniques require less number of session as compared to the spray technique. They have also observed that lower mass flow rate of cryogen is responsible for a longer duration of the treatment. Sehdev et al. [55] and Ahlgrimm-Siess et al. [59] have used multiple freeze thaw cycles for the treatment of planter warts and Basal cell carcinoma (BCC) respectively. The influence of hole diameter and spraying distance on cryoablation is studied by Kumari et al. [6]. The results reveal that hole diameter has greater impact on cryoablation as compared to the spraying distance. It means cryoablation can be increased through device modification.

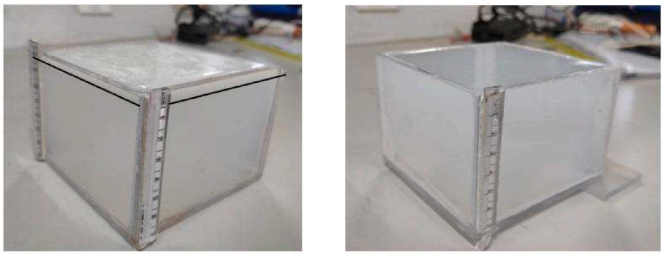

(a) Nano-phantom (b) Normal-phantom

Fig. 1. Phantoms used in the study.

As far as the scope of cryospray is concerned, there are studies that encourage the application of cryospray in the treatment of Bowen's disease, which is an intraepidermal squamous cell carcinoma (SCC) [28,58]. However, size and multiple or special anatomical sites of tumour prohibit its application in this field. Moreover, cryospray is a preferred method in the treatment of Barrett's esophagus [1,17,18,31,42] and port wine stain birthmark (PWS) [29,51,69]. It should be noted here that the motive of cryospray depends on the disease. In PWS treatment it is employed to reduce the localised heating of superficial skin caused by laser pulses whereas in the present case (cancer treatment) and Barrett's esophagus it is used to destruct the lesion occurring on the superficial skin and esophagus respectively. Aguilar et al. [20–22] have customised cryogen spray nozzles while changing their length and diameter to increase the amount of cooling. They concluded that narrow nozzles (d = 0.7 mm) produces fine spray as compared to wide nozzle (d = 1.4 mm). They further reported that wide nozzles have more heat extraction capacity than narrow nozzles.

Thus, acknowledging the advancement in transdermal drug delivery systems which leads to promising results of nanoparticle administration through stratum corneum [27,40]. The motive of the research is to explore an adjuvant assisted approach to increase the efficacy of cryospray. The reason behind the administration of adjuvant in the lesion is to improve the thermophysical properties of the lesion which will increase the rate of heat transfer in the lesion and decrease the duration of treatment. Moreover, larger lesions can also be treated through the proposed approach. It has been observed in the previous study that device modifications can eliminate the existing limitation of cryospray process [46,47]. Hence, customised multihole nozzles (MHN) compatible with commercial cryogun is used to spray the cryogen on adjuvant loaded phantom in the present study.

2. Materials and method

The Magnesium Oxide nanoparticles are used as adjuvant in the present study. A tissue phantom is prepared using agarose powder (Low EEO, HIMEDIA Chemicals, CAS: 9012-36-6, catalogue no. MB002-500G). The normal-phantom is made as per the procedure followed in the previous study [47]. Nano-phantom is made using the Magnesium Oxide (MgO) nanoparticles procured from Adnano Technologies. A mixture of surfactant span 20 (CAS No: 1338-39-2) 5% w/v, double distilled water (200 ml) and nanoparticles 0.2% w/v is stirred for 45 min with the help of magnetic stirrer at 900 rpm. Further, the prepared mixture is sonicated at 20 kHz for 60 min in the bath sonication. Agarose is added afterwards to form an adjuvant loaded gel. The solution is heated in the microwave oven at 900 W for 3 min. In order to mimic the actual conditions, layered phantom is made because studies of transdermal drug delivery suggest accumulation of drug in the vicinity of area of application [4,26]. Furthermore, the penetration of drug depends on the amount and the duration of dosing. Therefore, two layers are made in nano-phantom. The top layer comprises of agarose gel loaded with

Table 1
Nozzle geometry.

Schematic Diagram of MHN	Nomenclature
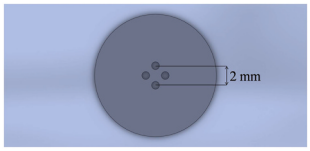	4A
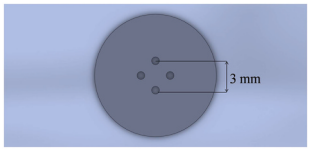	4B
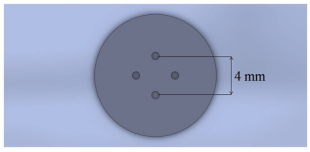	4C
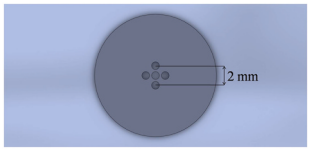	5A
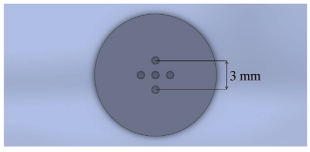	5B
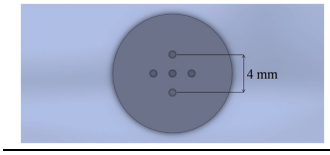	5C

nanoparticles whereas the bottom layer is made of agarose gel only. The thickness of top layer is taken as 5 mm to replicate the thickness of human skin [14]. A sample of normal-phantom and nano-phantom is shown in Fig. 1↓.

A commercial cryogun (CS-1) procured from SMT Praha, Czech Republic is used to spray the cryogen. Six customised MHNs are used in the present study to demarcate the impact of nozzle geometry on cryoablation. The orientation of holes in MHNs are shown in Table 1↑. Further specification of MHNs can be found elsewhere [46]. The diameter of each hole is 0.8 mm. Liquid nitrogen is used as the cryogen in the present case due to its lower boiling point (−196 °C) and non-toxic nature. The position of thermocouples and the design of experimental setup are kept same as in the previous study [46]. The location of thermocouples inside the phantom is shown in Fig. 2↓ .

3. 3 characterisation of nanofluid

The purity of MgO nanoparticles are confirmed through the XRD results (refer Fig. 3b↑). It clearly exhibits the peaks at angle 18.57°, 36.96°, 42.98°, 62.36°, 74.71° and 78.66° corresponding to (0 0 1), (1 1 1), (2 0 0), (2 2 0), (3 1 1) and (2 2 2) planes. It reflects that MgO nanoparticles possess cubic structure without any impurity phase [23,37]. The diffusion and transport of nanoparticles in skin depends on the size of nanoparticles [4,45]. Studies suggest that the particle size less than 40 nm can penetrate easily in the human skin [8,19]. The TEM images of MgO nanoparticles are shown in Fig. 3a↑. It can be seen in the image that particle size is less than 40 nm, so smooth penetration of particles can be ensured. A digital pH meter is used to measure the pH of nanofluid in order to verify the stability of nanofluid. If pH of nanofluid is far away from the isoelectric point (IEP) then its stability can be ensured. The observed IEP signifies that nanoparticles carry no charge, hence the zeta potential of solid is zero [53]. It causes reduction in electrostatic force of repulsion and agglomeration of nanoparticles due to the van der Waals force of attraction [52]. The IEP of MgO nanoparticle is 10.5 [60] whereas the pH of MgO nanofluid is 8.5, which means the nanofluid is stable.

The nanoparticles as adjuvants improve the thermal conductivity of the nano-phantom; hence, diffusion of heat in nano-phantom increases. The Hot Disk TPS 500 Thermal Constants Analyser is used to determine the thermal conductivity of the manufactured nano-phantom and normal-phantom. The thermal conductivity is found to be 0.71 ± 0.01 W/mK for nano-phantom and 0.59 ± 0.02 W/mK for the normal-phantom.

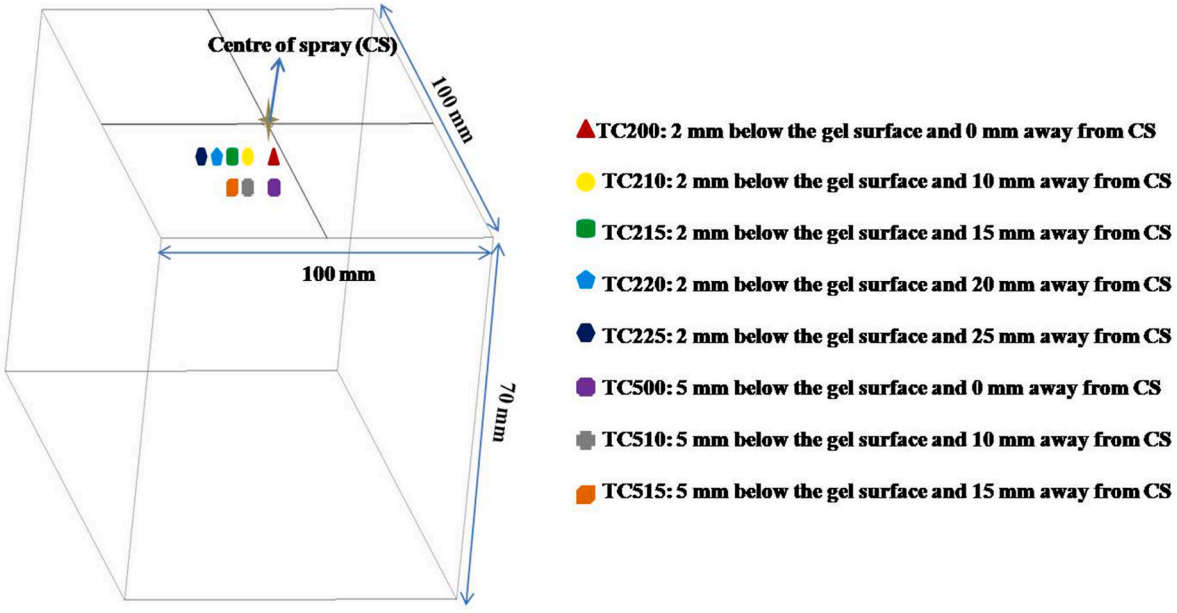

Fig. 2. Position of thermocouple.

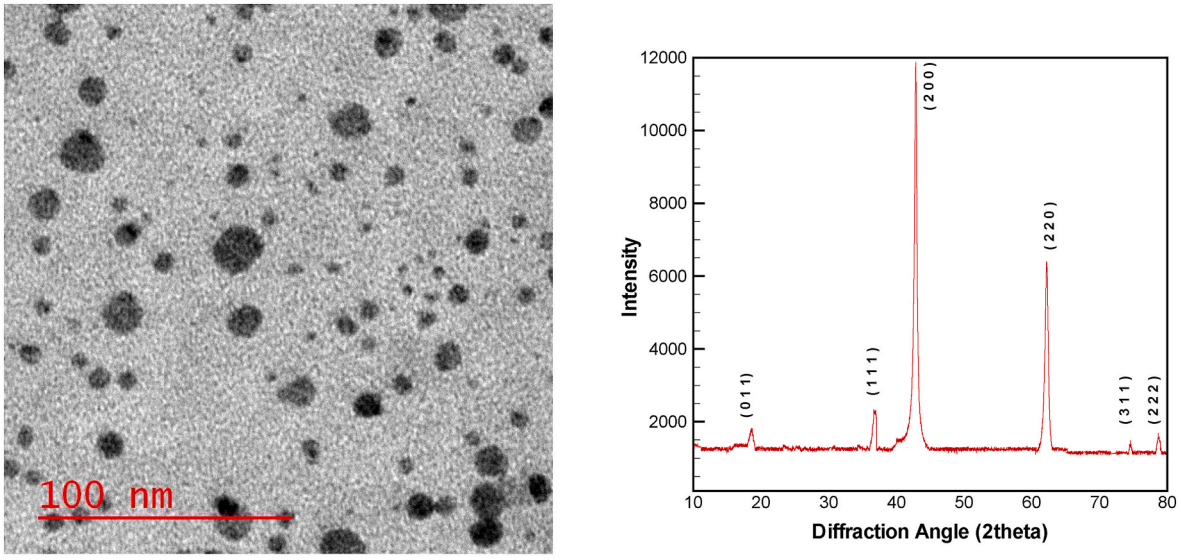

(a) TEM Images of MgO nanoparticles (b) XRD pattern of MgO nanoparticles

Fig. 3. Characterisation of nanoparticles.

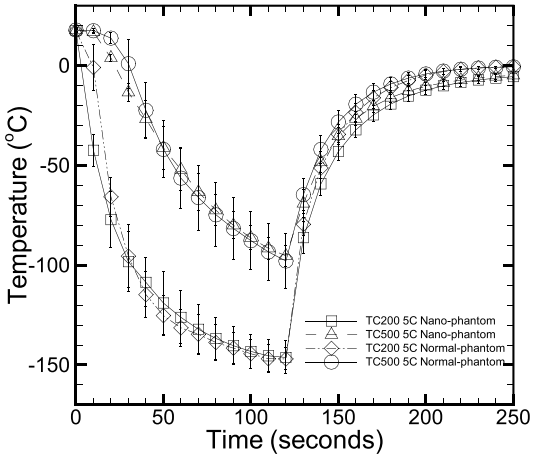

Fig. 4. 2 mm and 5 mm below the gel surface and 0 mm away from CS with 95% confidence interval for MHN 5C.

4. Results and discussion

To determine the influence of adjuvant in cryospray process, two different tissue phantoms namely nano-phantom and normal phantoms are made. Altogether 6 MHNs are selected to spray cryogen on different phantoms with a freezing cycle of 120 s followed by a natural thawing. The spraying distance is taken as 18 mm in the present study because it is the most effective spraying distance for MHNs [46,47].

4.1. Uncertainty analysis

The uncertainty in temperature measurement arises due to the two sources: stochastic uncertainty and the systematic uncertainty [43,61]. Systematic uncertainty accounts for the variation in temperature measurement due to the device, i.e. thermocouple, whereas random variations during experiment are acknowledged under stochastic uncertainty. The error in temperature measurement due to thermocouple is estimated to be 2 °C [33]. In order to ascertain the role of random parameters like manual interference and natural convention currents, each experiment is conducted 5 times. The stochastic uncertainty is calculated using student t-test. Fig. 4↓ represents the transient temperature variation for MHN 5C at TC200 and TC500 locations. The error bars shown in Fig. 4↓ are at 95% confidence interval. An overall uncertainty in temperature measurement is found to be ±15 °C. The experimental studies of cryospray and cryosurgery have reported the uncertainty of ±10 °C to ±15 °C in the temperature measurement [5,10,41,47]. Thus, it can be accepted for the present case.

4.2. Axial temperature distribution

The temperature distribution in nano-phantom at different axial locations is shown in Fig. 5↓ and Fig. 6↓. At.

TC200 location, as the margin among the holes increases the end temperature increases. The end temperatures obtained by MHNs 5A, 5B and 5C are −158 °C, −146 °C and −144 °C whereas −157 °C, −145 °C and −128 °C are the end temperatures obtained from MHNs 4A, 4B and 4C respectively. Table 2↓ lists the difference in the end temperatures of the nano-phantom and the normal-phantom.

The entries of Table 2↑ suggest similar observations in normal phantom, because appreciable difference in end temperature of nano-phantom and normal-phantom is not observed. It also reflects that the role of adjuvants in cryoablation is less pronounced at TC200 location. At TC210 location, MHNs with 5 holes follow similar trend in the temperature variation with respect to time as the margin among the holes increases. However in the case of MHNs with 4 holes, 4B registers the lowest end temperature followed by 4A and 4C respectively. The end temperatures registered by MHNs 5A, 5B, 5C, 4A, 4B and 4C are −142 °C, −138 °C, −129 °C, −113 °C, −123 °C and −113 °C respectively. Moreover, at TC210 location, scenario of difference in end temperature of nano-phantom and normal-phantom is quite different from the former location (TC200). An appreciable difference in the end temperature is registered by each MHN; MHNs 5A and 4B record highest difference in their respective categories. An enhanced thermal conductivity and a reduced specific heat of nano-phantom are the reasons for such variation [11]. Apart from that, the effect of margin among the holes on cryoablation can be ascertained from the temperature readings of MHNs with 4 holes at TC210 location in nano-phantom. The MHN 4B continues to provide maximum cooling in case of MHNs with 4 holes at TC215 location whereas in the case of MHNs with 5 holes, 5B provides the lowest end temperature than MHNs 5A and 5C respectively. The trends of end temperature at TC210 and TC215 locations indicate the role of margin among the holes and the central hole in cryoablation. The

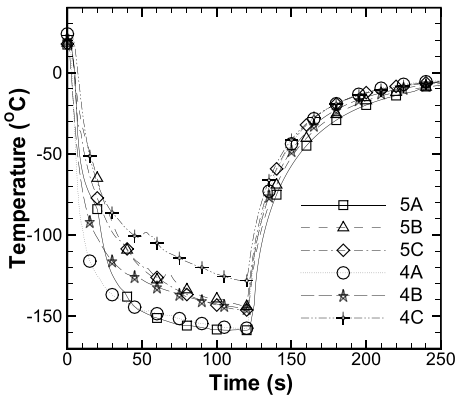

(a) 2 mm below gel surface and 0 mm away from centre of spray (TC200 location)

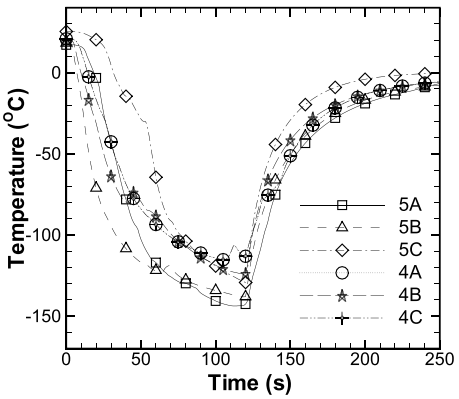

(b) 2 mm below gel surface and 10 mm away from centre of spray (TC210 location)

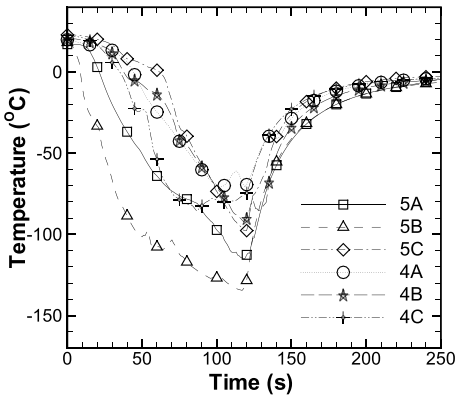

(c) 2 mm below gel surface and 15 mm away from centre of spray (TC215 location)

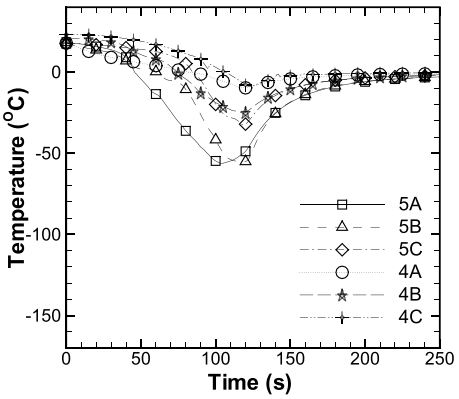

(d) 2 mm below gel surface and 20 mm away from centre of spray (TC220 location)

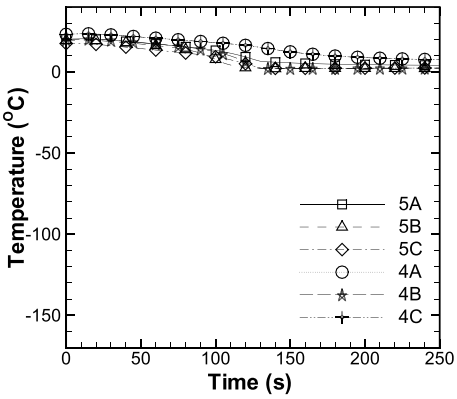

(e) 2 mm below gel surface and 25 mm away from centre of spray (TC225 location)

Fig. 5. Transient temperature curves of thermocouples placed at 2 mm below the gel surface and at different radial locations.

effect of margin is observed near the centre of the spray (at TC210 location) in the case of MHN with 4 holes whereas in the case of MHN with 5 holes, it is observed at TC215 location. The presence of central hole can be the reason for such behavior. Due to the presence of the central hole, mass flow rate of cryogen increases and the rate of evaporation from each individual jet reduces, thus larger droplets (in terms of diameter) strike the phantom surface which causes the formation of larger spray zone on the phantom surface. Therefore, in MHNs with 5 holes, the influence of margin is obtained away from the centre of the spray than in the MHNs with 4 holes. Similarly, −48 °C, −55 °C, −32 °C, −9 °C, −24 °C and −27 °C are the end temperatures registered by MHNs 5A, 5B, 5C, 4A, 4B and 4C respectively at TC220 location. It is important to mention here that freezing is not observed at TC225 location. Moreover, it is interesting to note here that as the distance from the centre of

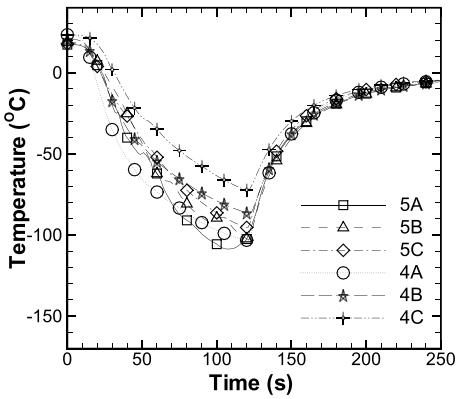

(a) 5 mm below gel surface and 0 mm away from centre of spray (TC500 location)

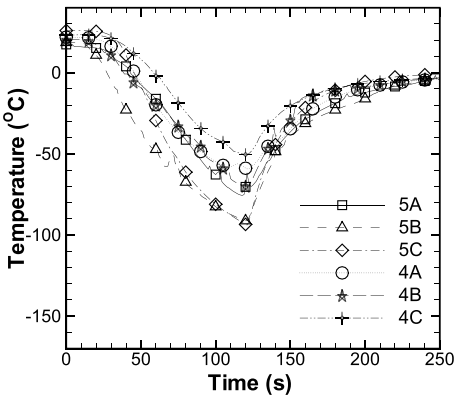

(b) 5 mm below gel surface and 10 mm away from centre of spray (TC510 location)

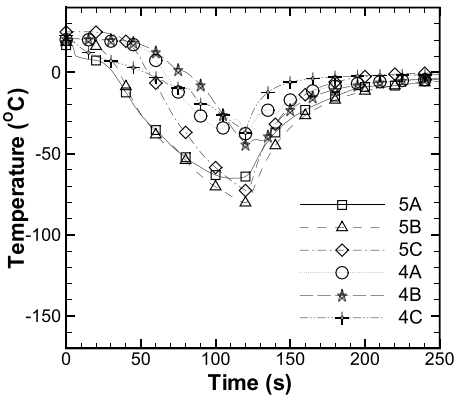

(c) 5 mm below gel surface and 15 mm away from centre of spray (TC515 location)

Fig. 6. Transient temperature curves of thermocouples placed at 5 mm below the gel surface and at different radial locations.

Table 2
Difference in end temperature of nano-phantom and normal-phantom [46].

Position of thermocouple	5A	5B	5C	4A	4B	4C
TC200	4	1	1	4	4	5
TC210	31	13	4	8	51	36
TC215	59	53	15	48	72	56
TC220	53	59	35	15	28	16
TC225	9	17	7	1	10	0
TC500	1	7	5	6	3	11
TC510	6	14	23	18	24	27
TC515	36	33	31	39	50	51

the spray increases, the difference between the end temperatures of nano-phantom and normal-phantom increases (refer Table 2↑). It reflects that adjuvant assisted approach increases cryoablation in the peripheral region of the spray zone. Similar observation is reported by Yan and liu [30]; they concluded that intentional loading of nanoparticles in tissue can lower the end temperature and increase the area of cryoablation. The thermocouples placed at 5 mm below the gel surface replicate the trends of end temperature as followed by thermocouples placed at 2 mm below the gel surface. A lower end temperature in nano-phantom is obtained at each location compared to the normal-phantom. Among the 6 MHNs selected in the study, MHNs 5B and 4B provide the most optimised result in terms of cryoablation in their respective categories.

Table 3
Cooling rate (^{0}C/min) of nano-phantom and normal-phantom [46].

Position of thermocouple	Nano-phantom						Normal-phantom					
	5A	5B	5C	4A	4B	4C	5A	5B	5C	4A	4B	4C
TC200	79	72	73	78	72	64	77	73	72	76	70	61
TC210	71	69	64	56	61	56	55	62	62	52	36	38
TC215	56	64	52	34	51	37	26	37	41	10	9	9
TC220	24	27	16	4	12	3	–	–	1	–	–	–
TC225	–	–	–	–	–	–	–	–	–	–	–	–
TC500	61	61	47	51	43	36	50	47	45	48	44	30
TC510	35	45	46	29	34	25	32	38	35	20	22	11
TC515	32	40	36	17	22	18	14	23	20	–	–	–

"-" Freezing of gel is not observed.

Table 4
Movement of lethal front and freezing front (in mm) on the gel surface after 120 s of spray.

Multihole Nozzle	Nano-phantom		Normal-phantom	
	Lethal front	Freezing front	Lethal front	Freezing front
5A	43	78	34	50
5B	42	82	30	50
5C	41	80	32	46
4A	36	80	32	46
4B	36	74	30	45
4C	34	72	28	42

The estimation of necrosis on the basis of lethal temperature provides its quantitative analysis whereas qualitative analysis requires the data of cooling rate [10,41,50]. The cooling rate governs the mechanism of necrosis. Studies suggest that formation of interacellular ice (IIF) ball as the main cause of cell destruction [25]. The cooling rate required for IIF varies from 50 to 200 °C/min; above 200 °C/min destruction rate decreases due to the vitrification of the cell. Table 3↓ lists the cooling rate for nano-phantom and normal-phantom at the discrete locations of thermocouple. It can be interpreted through the entries of Table 3↓ that the presence of adjuvants increases the zone of IIF.

In case of normal-phantom, IIF is observed up to TC210 location for MHNs with 5 holes whereas in nano-phantom, IIF is observed with each nozzle. It reflects that the adjuvants assist in the rapid diffusion of coldness. Similarly, at TC215 location, IIF is not observed with any MHN in normal-phantom whereas it is observed in nano-phantom (for MHNs with 5 holes). Furthermore, cooling rate is increased at each location in the case of nano-phantom. As per the observation of Rubinsky [3], cooling below lethal temperature guarantees cell death but cell death can also be assured above lethal temperature if that area falls under the specific range of cooling rate. The accepted range of lethal temperature, i.e. temperature required for the destruction of lesion, is −40 °C for a malignant tumour and −20 °C for a benign tumour [5,7,16,32,54]. Extracellular ice formation (EIF) is the dominant mechanism of cellular destruction in such regions. It forms when cooling rate is below 50 °C/min and considered as less lethal. So, necrosis can be assured at TC215, TC510 and TC515 locations through EIF in the nano-phantom. Thus, it can be concluded that the presence of adjuvant has increased the necrosis both quantitatively and qualitatively.

4.3. Radial temperature distribution

Table 4↓ represents the diameter of lethal front (temperature < −40 °C) and freezing front (temperature <0 °C) formed on the surface of nano-phantom and normal-phantom. The thermal images obtained after 30 s and 120 s of spray for MHN 5C in case of nano-phantom are shown in Fig. 7↓

The upper limit of the contour depicts the maximum temperature in the domain, i.e. temperature of human hand whereas the lower limit depicts −40 °C which is not the minimum temperature of the domain. The thermal imaging camera operates in the range of −40 °C to 120 °C, so the minimum temperature it can capture is −40 °C. However, the actual temperature in those regions can be much lower than −40 °C. The study regarding authentication of thermal images can be found elsewhere [46]. The thermal images are captured through FLIR E75 thermal imaging camera. The data extraction technique followed in the previous studies [46,47] is used to extract the data from thermal images. The dimensions of lethal front and freezing front are larger in nano-phantom than in the normal-phantom. Nanoparticles promote heterogeneous ice formation by reducing the degree of supercooling of the nano-phantom thereby assisting in the formation of larger ice ball [15,44]. Moreover, hydrophilic nature of MgO nanoparticles facilitates the nucleation of ice by decreasing the Gibbs free energy [62,64,68]. The entries of Table 4↑ suggest that in case of nano-phantom, as the margin among the holes increases the area of necrotic zone reduces in MHNs with 5 holes. Moreover, MHNs with 4 holes follow the similar trend. It should be noted here that as the margin among the holes increases the spray zone of cryogen increases but the cooling capacity decreases which can be attributed as a reason to such variation. The cooling capacity decreases because the distance between each individual jet increases leading to more evaporation of cryogen during its flight from the nozzle exit to the phantom surface due to the entertainment of ambient air. On the basis of radial temperature distribution, MHN 5A provides the most optimised result among the 6 nozzles selected in the study and MHN 4B provides the maximum cryobalation in MHNs with 4 holes. The area of necrotic zone of 5A, 5B and 5C is 59%, 96% and 64% larger in nano-phantom than in the normal-phantom respectively. Similarly, the area of necrotic zone in nano-phantom is 26%, 44% and 30% larger than in normal-phantom for 4A, 4B and 4C respectively. The diameter of freezing front is almost twice larger than the diameter of lethal front in nano-phanotm for each MHN whereas such trend is not observed in the normal-phantom. It reflects that the energy diffusion ability of agarose gel increases with the presence of nanoparticles.

5. Conclusion

The present study deals with increasing the rate of heat transfer inside the lesion through the modification in the spraying technique (MHN) as well as the thermophysical properties of the lesion (adjuvants). It has been observed that with the proposed approach, the necrosis of lesion with a diameter of 10 mm and an axial depth of 2 mm can

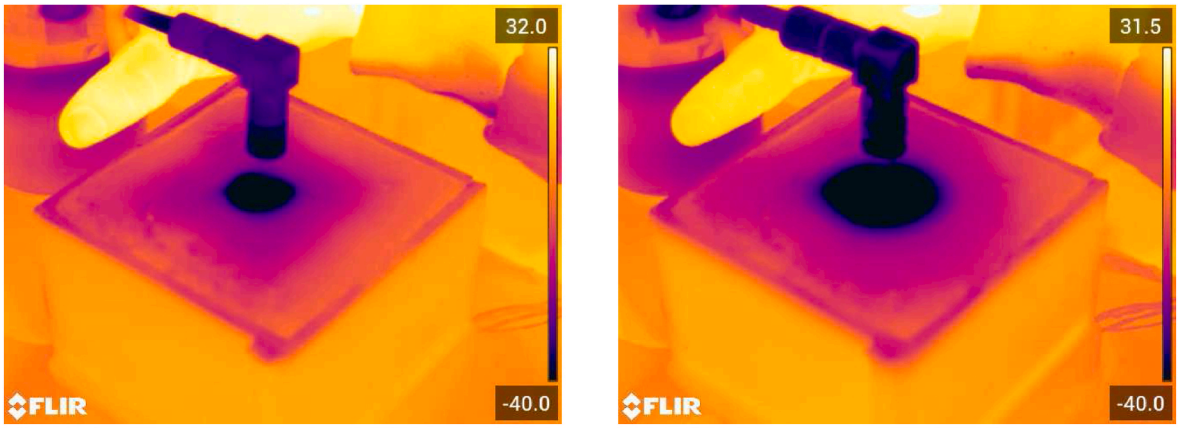

(a) After 30 s of spray on nano-phantom (b) After 120 s of spray on nano-phantom

Fig. 7. Temperature contour on the surface of gel when MHN 5C is used to spray cryogen for reference purpose.

be achieved within 15 s of spray (for MHN 5B) whereas it cannot be achieved even after 120 s of spray through the conventional technique for the same spraying distance. The conventional technique refers to a case where commercial single hole nozzle (SHN) of 0.8 mm diameter is used to spray cryogen on normal-phantom. The influence of adjuvant on cryoablation is quatified while spraying cryogen with different MHNs on nano-phantom and normal-phantom respectively. It has been ascertained that the necrosis of lesion with a diameter of 15 mm and an axial depth 2 mm is achieved within 23 s of spray in nano-phantom whereas it is achieved after 96 s of spray in normal-phantom when MHN 5B is used to spray the cryogen. It means that the rate of heat diffusion has increased inside the phantom due to the presence of adjuvant. Furthermore, the area of cryoablation in nano-phantom is more than 60% larger than that in the normal-phantom after 120 s of spray when cryogen is sprayed through a MHN with 5 holes. Interacellular ice formation is predicted up to a radius of 15 mm from the centre of the spray at an axial depth of 2 mm for MHNs with 5 holes. However, it decreased to a radius of 10 mm from the centre of the spray at an axial depth of 2 mm for MHNs with 4 holes. Among the six MHNs used in the study, MHN 5B provided the most optimised result in terms of cryoablation. Such approach can be useful in the treatment of larger lesions like keloids and Squamous cell carcinoma.

Declaration of competing interest

The authors declare that they have no known competing financial interests or personal relationships that could have appeared to influence the work reported in this paper.

Data availability

No data was used for the research described in the article.

Acknowledgment

The work carried out is a part of the project sponsored by DIC-IIT (BHU), Varanasi, India.

References

[1] A.M. Chen, P.J. Pasricha, Cryotherapy for barrett's esophagus: who, how, and why? Gastrointestinal Endoscopy Clinics of North America 21 (1) (2011) 111–118. Advances in the Diagnosis and Management of Barrett's Esophagus, http://www.sciencedirect.com/science/article/pii/S1052515710001261.
[2] B. Mourad, N. Elfar, S. Elsheikh, Spray versus intralesional cryotherapy for keloids, J. Dermatol. Treat. 27 (3) (2015) 264–269.
[3] B. Rubinsky, Cryosurgery, Annu. Rev. Biomed. Eng. 2 (2000) 157–187.
[4] Baeckkyoung Sung, Minsoo Kim, Min Su Kim, Jin-Kyu Lee, Kwang-Sup Soh, Quantitative real-time imaging of nanofluid convection—diffusion in the planar skin layer in vivo, Biomed. Phy. Eng. Ex. 3 (1) (2017), 015024, https://doi.org/10.1088/2057-1976/aa5949.
[5] C.C. Rupp, N.E. Hoffmann, F.R. Schmidlin, D.J. Swanlund, J.C. Bischof, J.E. Coada, Cryosurgical changes in the porcine kidney: histologic analysis with thermal history correlation, Cryobiology 45 (2002) 167–182.
[6] C. Kumari, A. Kumar, S.K. Sarangi, A. Thirugnanam, Effects of spray parameters on skin tumour ablation volume during cryotherapy, Australas. Phys. Eng. Sci. Med. 42 (2019) 453–464.
[7] C. Zouboulis, Priniples of cutaneous cryosurgery, An Update Dermatol. 198 (1999) 111–117.
[8] Ai-Zheng Chen, Lin-Qing Chen, Shi-Bin Wang, Ya-Qiong Wang, Jun-Zhe Zha, Study of magnetic silk fibroin nanoparticles for massage-like transdermal drug delivery, Int. J. Nanomed. 10 (2015) 4639–4651. URL, https://europepmc.org/articles/PMC4516257.
[9] Chitta Ranjan Patra, Resham Bhattacharyaa, Priyabrata Mukherjee, Fabrication and functional characterization of goldnanoconjugates for potential application in ovarian cancer, J. Mater. Chem. 20 (3) (2010) 547–554, https://doi.org/10.1039/b913224d.
[10] K.J. Chua, S.K. Chou, On the study of the freeze thaw thermal process of a biological system, Appl. Therm. Eng. 29 (2009) 3696–3709.
[11] D. Cabaleiro, C. Gracia-Fernandez, J.L. Legido, L. Lugo, Specific heat of metal oxide nanofluids at high concentrations for heat transfer, Int. J. Heat Mass Tran. 88 (2015) 872–879. https://www.sciencedirect.com/science/article/pii/S0017931015004780.
[12] D.E. Rowe, R.J. Carroll, C.L. Day, Prognostic factors for local recurrence, metastasis, and survival rates in squamous cell carcinoma of the skin, ear, and lip: implications for treatment modality selection, J. Am. Acad. Dermatol. 26 (6) (1992) 976–990. http://www.sciencedirect.com/science/article/pii/0190962292701445.
[13] D. Papakostas, F. Rancan, W. Sterry, U. Blume-Peytavi, A. Vogt, Nanoparticles in dermatology, Arch. Dermatol. Res. 303 (2011) 533–550.
[14] D. Sarkar, A. Haji-Sheikh, A. Jain, Temperature distribution in multi-layer skin tissue in presence of a tumor, Int. J. Heat Mass Tran. 91 (2015) 602–610.
[15] De-Rui Di, Zhi-Zhu He, Zi-Qiao Sun, Jing Liu, A new nano-cryosurgical modality for tumor treatment using biodegradable MgO nanoparticles, Nanomed. Nanotechnol. Biol. Med. 8 (8) (2012) 1233–1241. http://www.sciencedirect.com/science/article/pii/S154996341200086X.
[16] E.G. Kuflik, Cryosurgery updated, J. Am. Acad. Dermatol. 31 (1994) 925–944.
[17] F.B. Peng, A.C. Elden, B. Shinn, J. Spataro, D.M. Kastenberg, C. Tofani, A. Infantolino, Does multifocal dysplasia in barretts esophagus increase the risk of progression to esophageal adenocarcinoma? Am. J. Gastroenterol. 113 (2018).
[18] F.H. Ramay, Q. Cui, B.D. Greenwald, Outcomes after liquid nitrogen spray cryotherapy in Barrett's esophagus-associated highgrade dysplasia and intramucosal adenocarcinoma: 5-year follow-up, Gastrointest. Endosc. 86 (4) (2017) 626–632.
[19] Francesca Larese Filon, Marcella Mauro, Gianpiero Adami, Massimo Bovenzi, Matteo Crosera, Nanoparticles skin absorption: new aspects for a safety profile evaluation, Regul. Toxicol. Pharmacol. 72 (2) (2015) 310–322. https://www.sciencedirect.com/science/article/pii/S027323001500104X.
[20] G. Aguilar, B. Majarom, W. Verkruysse, Y. Zhou, J.S. Nelson, E.J. Lovernia, Theoretical and experimental analysis of droplet diameter, temperature and evaporation rate evolution in cryogenic sprays, Int. J. Heat Mass Tran. 44 (2001) 3201–3211.
[21] G. Aguilar, B. Majaron, E. Karapetian, E.J. Lavernia, J.S. Nelson, Experimental study of cryogen spray properties for application in dermatologic laser surgery, IEEE (Inst. Electr. Electron. Eng.) Trans. Biomed. Eng. 50 (7) (2003) 863–869.
[22] G. Aguilar, W. Verkruysse, B. Majaron, L.O. Svaasand, E.J. Lavernia, J.S. Nelson, Measurement of heat flux and heat transfer coefficient during continuous cryogen spray cooling for laser dermatologic surgery, IEEE J. Sel. Top. Quant. Electron. 7 (6) (2001) 1013–1021.
[23] G. Balakrishnan, R. Velavan, Khalid Mujasam Batoo, Emad H. Raslan, Microstructure, optical and photocatalytic properties of MgO nanoparticles, Results Phys. 16 (2020), 103013. https://www.sciencedirect.com/science/article/pii/S221137971933493X.
[24] R. Goel, K. Anderson, J. Slaton, F. Schmidlin, G. Vercellotti, J. Belcher, J.C. Bischof, Adjuvant approaches to enhance cryosurgery, J. Biomech. Eng. 131 (2009) 1–11.
[25] H. Takeda, S. Maruyama, J. Okajima, S. Aiba, A. Komiya, Development and estimation of a novel cryoprobe utilizing the Peltier effect for precise and safe cryosurgery, Cryobiology 59 (2009) 275–284.
[26] Issei Takeuchi, Yosuke Shimamura, Yuki Kakami, Tsunenori Kameda, Keitaro Hattori, Seiji Miura, Hiroyuki Shirai, Mutsuo Okumura, Toshio Inagi, Hiroshi Terada, Kimiko Makino, Transdermal delivery of 40-nm silk fibroin nanoparticles, Colloids Surf. B Biointerfaces 175 (2019) 564–568. http://www.sciencedirect.com/science/article/pii/S0927776518308944.
[27] J.J. Escobar-Chavez, R. Diaz-Torres, I.M. Rodríguez-Cruz, C.L. Dominguez-Delgado, R.S. Morales, E. Angeles-Anguiano, L.M. Melgoza-Contreras, Nanocarriers for Transdermal Drug Delivery", vol. I, Dove Medical Press Ltd, 2020, pp. 3–17.
[28] J.M. Peikert, Prospective trial of curettage and cryosurgery in the management of non-facial, superficial, and minimally invasive basal and squamous cell carcinoma, Int. J. Dermatol. 50 (2011) 1135–1138.
[29] Jia-Meng Tian, Bin Chen, Zhi-Fu Zhou, Parametric effect investigation on surface heat transfer performances during cryogen spray cooling, Appl. Therm. Eng. 143 (2018) 767–776. http://www.sciencedirect.com/science/article/pii/S1359431118329661.
[30] Jing-Fu Yan, Jing Liu, Nanocryosurgery and its mechanisms for enhancing freezing efficiency of tumor tissues, Nanomed. Nanotechnol. Biol. Med. 4 (1) (2008) 79–87. http://www.sciencedirect.com/science/article/pii/S154996340700247X.
[31] K. Visrodia, L. Zakko, S. Singh, C.L. Leggett, P.G. Iyer, K.K. Wang, Cryotherapy for persistent Barrett's esophagus after radiofrequency ablation: a systematic review and meta-analysis, Gastrointest. Endosc. 87 (6) (2018) 1396–1404, e1, http://www.sciencedirect.com/science/article/pii/S0016510718301354.
[32] K.J. Chua, S.K. Chou, J.C. Ho, An analytical study on the thermal effects of cryosurgery on selective cell destruction, J. Biomech. 40 (2007) 100–116.
[33] K.K. Ramajayam, A. Kumar, S.K. Sarangi, A. Thirugnanam, Adjuvant-perfluorocarbon based approach for improving the effectiveness of cryosurgery in gel phantoms, Int. J. Therm. Sci. 132 (2018) 296–308. http://www.sciencedirect.com/science/article/pii/S1290072917305215.
[34] Karthikeyan Krishnamoorthy, Jeong Yong Moon, Ho Bong Hyun, Somi Kim Cho, Sang-Jae Kim, Mechanistic investigation on the toxicity of MgO nanoparticles toward cancer cells, J. Mater. Chem. 22 (2012) 24610–24617, https://doi.org/10.1039/C2JM35087D.
[35] M. Andrews, Cryosurgery for common skin conditions, Am. Fam. Physician 69 (2004) 2365–2372.
[36] M.R. Prausnitz, R. Langer, Transdermal drug delivery, Nat. Biotechnol. 26–11 (2008) 1261–1268.
[37] M.R. Bindhu, M. Umadevi, M. Kavin Micheal, Mariadhas Valan Arasu, Naif Abdullah Al-Dhabi, Structural, morphological and optical properties of MgO nanoparticles for antibacterial applications, Mater. Lett. 166 (2016) 19–22. https://www.sciencedirect.com/science/article/pii/S0167577X15309721.

[38] Mariappan Premanathan, Krishnamoorthy Karthikeyan, Kadarkaraithangam Jeyasubramanian, Govindasamy Manivannan, Selective toxicity of ZnO nanoparticles toward Gram-positive bacteria and cancer cells by apoptosis through lipid peroxidation, Nanomed. Nanotechnol. Biol. Med. 7 (2) (2011) 184–192. https://www.sciencedirect.com/science/article/pii/S1549963410003527.

[39] Mark R. Prausnitz, Microneedles for transdermal drug delivery, Adv. Drug Deliv. Rev. 56 (5) (2004) 581–587. Breaking the Skin Barrier, https://www.sciencedirect.com/science/article/pii/S0169409X03002394.

[40] Muhammad Azam Tahir, Mohamed Ehab Ali, Alf Lamprecht, Nanoparticle formulations as recrystallization inhibitors in transdermal patches, Int. J. Pharm. 575 (2020), 118886. http://www.sciencedirect.com/science/article/pii/S0378517319309317.

[41] N.E. Hoffmann, J.C. Bischof, Cryosurgery of normal and tumor tissue in the dorsal skin flap chamber: part I-thermal response, J. Biomech. Eng. 123 (2001), 310-309.

[42] N.J. Shaheen, B.D. Greenwald, A.F. Peery, J.A. Dumot, N.S. Nishioka, H. C. Wolfsen, J.S. Burdick, J.A. Abrams, K.K. Wang, D. Mallat, M.H. Johnston, A. M. Zfass, J.O. Smith, J.S. Barthel, C.J. Lightdale, Safety and efficacy of endoscopic spray cryotherapy for Barrett's esophagus with high-grade dysplasia, Gastrointest. Endosc. 71 (4) (2010) 680–685. URL, http://www.sciencedirect.com/science/article/pii/S0016510710000313.

[43] N.J. Thomas, Uncertainty Analysis of Thermocouple Measurements Used in Normal and Abnormal Thermal Environment Experiments at Sandia's Radiant Heat Facility and Lurance Canyon Burn Site, 2004.

[44] Naeem M. El-Sawy, Amany I. Raafat, Nagwa A. Badawy, Asmaa M. Mohamed, Radiation development of pH-responsive (xanthan-acrylic acid)/MgO nanocomposite hydrogels for controlled delivery of methotrexate anticancer drug, Int. J. Biol. Macromol. 142 (2020) 254–264. https://www.sciencedirect.com/science/article/pii/S0141813019333082.

[45] Nouf N. Mahmoud, Alaaldin M. Alkilany, Dorthe Dietrich, Uwe Karst, G. Amal, Al-Bakri, A. Enam, Khalil, "Preferential accumulation of gold nanorods into human skin hair follicles: effect of nanoparticle surface chemistry", J. Colloid Interface Sci. 503 (2017) 95–102. https://www.sciencedirect.com/science/article/pii/S0021979717305222.

[46] Prashant Srivastava, Amitesh Kumar, Characterization of performance of multihole nozzle in cryospray, Cryobiology 96 (2020) 197–206. https://www.sciencedirect.com/science/article/pii/S0011224020301322.

[47] Prashant Srivastava, Amitesh Kumar, Optimizing the spray parameters of a cryospray process, Cryobiology 98 (2021) 201–209. https://www.sciencedirect.com/science/article/pii/S0011224020303096.

[48] R. Khademi, D. Mohebbi-Kalhori, A. Razminia, Thermal analysis of a tumorous vascular tissue during pulsedcryosurgery and nano-hyperthermia therapy: finite element approach, Int. J. Heat Mass Tran. 137 (2019) 1001–1013.

[49] R. P. Usatine, D. L. Stulber, G. B. Colver, Cutaneous Cryosurgery, Principles and Clinical Practice. CRC Press, Taylor & Francis Group, .

[50] R.B. Colemana, R.N. Richardson, A novel closed cycle cryosurgical system, Int. J. Refrig. 28 (2005) 412–418.

[51] Rui Wang, Bin Chen, Xin-Sheng Wang, Numerical simulation of cryogen spray cooling by a three-dimensional hybrid vortex method, Appl. Therm. Eng. 119 (2017) 319–330.

[52] M. Sharifpur, S.A. Adio, J.P. Meyer, Factors affecting the pH and electrical conductivity of MgO-ethylene glycol nanofluids, Bulletin of Mateial Science 38–5 (2015) 1345–1357.

[53] S. Kittaka, Isoelectric point of Al2O3, Cr2O3 and Fe2O3. I. Effect of heat treatment, J. Colloid Interface Sci. 48 (2) (1974) 327–333. URL, https://www.sciencedirect.com/science/article/pii/0021979774901672.

[54] S. Singh, R. Bhargava, Simulation of phase transition during cryosurgical treatment of a tumor tissue loaded with nanoparticles using meshfree approach, J. Heat Tran. 136 (2014) 121101–121110.

[55] S. Singh, S. Neema, Comparison of Electrosurgery by Electrodessication versus Cryotherapy by Liquid Nitrogen Spray Technique in the Treatment of Plantar Warts, Medical Journal Armed Forces India, 2019. http://www.sciencedirect.com/science/article/pii/S0377123718301539.

[56] Sabine Szunerits, Rabah Boukherroub, Heat: a highly efficient skin enhancer for transdermal drug delivery, Front. Bioeng. Biotechnol. 6 (2018).

[57] Satya Prakash, Meenakshi Malhotra, Wei Shao, Catherine Tomaro-Duchesneau, Sana Abbasi, Polymeric nanohybrids and functionalized carbon nanotubes as drug delivery carriers for cancer therapy, Adv. Drug Deliv. Rev. 63 (14) (2011) 1340–1351. https://www.sciencedirect.com/science/article/pii/S0169409X11001876. Hybrid nanostructures for diagnostics and therapeutics.

[58] T. Neubert, P. Lehmann, Bowen's disease-a review of newer treatment options, Therapeut. Clin. Risk Manag. 4 (5) (2008) 1085–1095.

[59] V.A. Siess, M. Horn, S. Koller, R. Ludwig, A. Gerger, R.H. Wellenhof, Monitoring efficacy of cryotherapy for superficial basal cell carcinomas with in vivo reflectance confocal microscopy: a preliminary study, J. Dermatol. Sci. 53 (1) (2009) 60–64. http://www.sciencedirect.com/science/article/pii/S0923181108002557.

[60] Vivek Kumar, Jahar Sarkar, Experimental hydrothermal characteristics of minichannel heat sink using various types of hybrid nanofluids, Adv. Powder Technol. 31 (2) (2020) 621–631. https://www.sciencedirect.com/science/article/pii/S0921883119304261.

[61] W.G. Steele, P.K. Maciejewski, C.A. James, R.P. Taylor, H.W. Coleman, Asymmetric systematic uncertainties in the determination of experimental uncertainty, AIAA J. 34–7 (1996) 1458–1463.

[62] Wei Cui, Lisi Jia, Ying Chen, Yiang Li, Jun Li, Songping Mo, Supercooling of water controlled by nanoparticles and ultrasound, Nanoscale Res. Lett. 13 (2018), 145.

[63] X. Zhang, S.M.C. Hossain, Q. Wang, B. Qiu, G. Zhao, Two-phase flow and heat transfer in a self-developed MRI compatible LN2 cryoprobe and its experimental evaluation, Int. J. Heat Mass Tran. 136 (2019) 709–718.

[64] Xiang Yang Liu, Ning Du, Zero-sized effect of nano-particles and inverse homogeneous nucleation: principles of freezing and antifreeze, J. Biol. Chem. 279 (7) (2004) 6124–6131. https://www.sciencedirect.com/science/article/pii/S0021925820749525.

[65] Yi Hou, Ziqiao Sun, Wei Rao, Jing Liu, Nanoparticle-mediated cryosurgery for tumor therapy, Nanomed. Nanotechnol. Biol. Med. 14 (2) (2018) 493–506. http://www.sciencedirect.com/science/article/pii/S1549963417302149.

[66] T. Yu, J. Liu, Y. Zhou, Selective freezing of target biological tissues after injection of solutions with specific thermal properties, Cryobiology 50 (2005) 174–182.

[67] Z. Deng, J. Liu, Numerical simulation of selective freezing of target biological tissues following injection of solutions with specific thermal properties, Cryobiology 50 (2005) 183–192.

[68] Zhisen Zhang, Xiang-Yang Liu, Control of ice nucleation: freezing and antifreeze strategies, Chem. Soc. Rev. 47 (2018) 7116–7139, https://doi.org/10.1039/C8CS00626A.

[69] Zhifu Zhou, Weitao Wu, Bin Chen, Guoxiang Wang, Liejin Guo, An experimental study on the spray and thermal characteristics of R134a two-phase flashing spray, Int. J. Heat Mass Tran. 55 (15) (2012) 4460–4468. http://www.sciencedirect.com/science/article/pii/S0017931012002645.